SCIENTIFIC REPORTS

OPEN

SUBJECT AREAS:
CHEMICAL PHYSICS
THEORETICAL PHYSICS
PHYSICAL CHEMISTRY
ATOMIC AND MOLECULAR PHYSICS

Received
27 February 2012

Accepted
19 March 2012

Published
11 April 2012

Correspondence and requests for materials should be addressed to H.P.F. (fanghaiping@sinap.ac.cn)

Critical Dipole Length for the Wetting Transition Due to Collective Water-dipoles Interactions

Chunlei Wang[1], Bo Zhou[1,2], Yusong Tu[3], Manyi Duan[4], Peng Xiu[5], Jingye Li[1] & Haiping Fang[1,6]

[1]Labortory of Physical Biology and Division of Interfacial Water, Shanghai Institute of Applied Physics, Chinese Academy of Sciences, P.O. Box 800-204, Shanghai 201800, China, [2]Graduate School of the Chinese Academy of Sciences, Beijing 100080, China, [3]Institute of Systems Biology, Shanghai University, Shanghai, 200444, China, [4]School of Physical Science and Technology, Sichuan University, Chengdu, 610064, China, [5]Bio-X Lab, Department of Physics, Department of Engineering Mechanics, and Soft Matter Research Center, Zhejiang University, Hangzhou 310027, China, [6]Modern Mechanics Division, E-Institutes of Shanghai University, Shanghai, 200444, China.

The wetting behavior of water on the solid surfaces is fundamental to various physical, chemical and biological processes. Conventionally, the surface with charges or charge dipoles is hydrophilic, whereas the non-polar surface is hydrophobic though some exceptions were recently reported. Using molecular dynamics simulations, we show that there is a critical length of the charge dipoles on the solid surface. The solid surface still exhibited hydrophobic behavior when the dipole length was less than the critical value, indicating that the water molecules on the solid surface seemed not "feel" attractive interactions from the charge dipoles on the solid surface. Those unexpected observations result from the collective interactions between the water molecules and charge dipoles on the solid surface, where the steric exclusion effect between water molecules greatly reduces the water-dipole interactions. Remarkably, the steric exclusion effect is also important for surfaces with charge dipole lengths greater than this critical length.

A microscopic understanding of the wettability of solid surfaces is fundamental to various physical[1–20], chemical[21–27] and biological processes[28–33], such as microfluidics[34,35] and sensing[36,37]. Particularly, the hydrophobic effect plays a key role in protein folding[38–40], nano-scale dewetting transition[41–43] and self-assembly of amphiphiles[44,45]. However, the physics of the hydrophilic or hydrophobic effects is not fully understood because the hydrophilicity or hydrophobicity of a surface is usually subject to various factors, including temperature[46] and morphology[47]. Conventionally, the surface with charge dipoles is hydrophilic, whereas the non-polar surface is hydrophobic. However, some exceptions were recently reported. Zangi and Berne[48,49] showed that a high value (e.g., 1.5 e) of electrolyte particles in solution can induce hydrophobic particles to be more hydrophobic. Giovambattista *et al.*[50] performed a series of simulations on polar hydroxylated silica (Si-OH) surfaces, finding that the surface is macroscopically hydrophobic, even though the dipole moment magnitude equaled to 41% that of the water molecule. The topography of the surface was also found to play a significant role in the wetting behavior of the protein surface or hydroxylated silica surface[51,52]. Boron-nitrogen nanotubes with a partial charge of $\sim$0.4e[53] have been shown to still exhibit hydrophobicity[54]. Moreover, in 2006, Li *et al.*[55] showed that van der Waals interactions are the dominant interactions between the superhydrophobic surface molecule $CF_3(CF2)_x(CH2)_y$ and the water molecules on the surface with a charge of -0.2 e in CF_3 groups. Very recently, we showed that hydrophobic-like behavior occurs on extremely polar hexagonal surfaces due to the ordered water monolayer for very large partial charges[4,56], which was recently confirmed experimentally[57]. However, a relatively complete picture about the effect of the surface charges and charge dipoles on the wetting property is still lacking.

Here, using molecular dynamics simulations, we show that the length of the charge dipoles on the solid surface plays a key role on the wetting behavior. Moreover, there is a critical length of the charge dipoles on the solid surface, below which the charge dipoles on the solid surface plays unexpectedly negligible role in the wetting property. The solid surface still exhibits hydrophobic behavior when the dipole length is less than the critical value, indicating that the water molecules on the solid surface seem not to "feel" attractive interactions from the charge dipoles on the solid surface, no matter how large the moment magnitude of the charge dipoles is. Those unexpected observations result from the collective interactions between the water molecules and charge dipoles on the solid surface, where the steric exclusion effect between water molecules prevents those hydrogen atoms of

water molecules from staying very close to the negative charge and those oxygen atoms of water molecules from staying very close to the positive charge, reducing the interactions between the water molecules and the charge dipoles. Interestingly, the steric exclusion effect was also important for surfaces with charge dipole lengths greater than this critical length. When the charge dipole lengths are greater than this critical length, it is found that the surfaces become more hydrophilic with the dipole lengths increase. We note that the bond lengths of most of common materials are less than the critical lengths, suggesting that the observation should be of general importance to the surface wetting properties.

The geometry of the solid surface system is shown in Fig. 1(a,b) together with snapshots of some water molecules. Positive and negative charges of the same magnitude, q, were assigned to every bonding atom of the hexagonal arrangement, represented by green and blue triangles, respectively, which was similar to the graphene and boron-nitrogen monolayer. The surface was neutral. The length of charge dipoles was denoted as l. Initially, 924 water molecules in a rectangular shape were located on solid surface composed of 2376 atoms in a box. Each system was simulated by molecular dynamics (MD) for 10 ns, and the data of the last 2 ns were collected for analysis. For all simulations, the water slab was in phase-level coexistence with the vapor at 300 K.

Results

Generally, the existence of polarity on the surface enhances the hydrophilicity. Surprisingly, our simulation shows that the contact angles of the liquid water droplets on the solid surfaces are always close to, even larger than 90° when $l \leq 0.202$ nm, for all q value in the interval of [0, 1.0 e]. In Fig. 1(c), we show the contact angle discrepancy ($\theta_0 - \theta_q$) values associated with the parameter l for different q, where θ_q and θ_0 are the contact angles of the liquid droplets on the surface with the charge of q and without any charge, respectively. For $l \leq 0.202$ nm, θ_q is very close to θ_0 for all charges less than 1.0 e, indicating that the effect of the charge dipoles on the wetting property of the surface is negligible. From Fig. 1(c), one can observe that $\theta_0 - \theta_q$ increases as l increases from 0.202 nm. The larger the value of q, the faster $\theta_0 - \theta_q$ increases. The increase of $\theta_0 - \theta_q$ is very quick for $q \geq 0.6$ e, and it reaches its maximal value, which corresponds to the water completely wetting the solid surface ($\theta_q = 0$), for $q = 1.0$ e at $l \geq 0.242$ nm, for $q = 0.8$ e at $l \geq 0.262$ nm, and for $q = 0.6$ e at $l \geq 0.402$ nm. A longer dipole length is clearly required to achieve complete wetting of the solid surface for a smaller charge. However, we find that the water could not complete wet the solid surface for $q \leq 0.4$ e, even if l is very large (0.482 nm). Interestingly, for $q = 0.4$ e, the contact angle increases significantly only from $l \approx 0.3$ nm. Thus, the wetting properties of the solid surface significantly depend on the length of the dipole. We note that, when $l \leq 0.202$ nm, the surface always shows hydrophobic ($\theta_q \approx 90°$) when the dipole moment magnitude is very large, even larger than 3 times of that of the water molecule. In order to better characterize the behavior, we define a critical length as the dipole length below which the contact angle discrepancy ($\theta_0 - \theta_q$) is less than a critical value, i.e., 15°, for all q value in the interval of [0, 1.0 e], or in the interval of [0, 0.4 e], denoted by l_C and $l_C^{0.4}$, respectively. $l_C = 0.202$ nm and $l_C^{0.4} = 0.302$ nm, which are shown by grey and light blue shadows in Fig. 1(c), respectively. We note the bond lengths of many common materials are smaller than $l_C = 0.202$ nm and most of common materials are smaller than $l < l_C^{0.4} = 0.302$ nm (see Fig. 1d and the Table S1 in the Supporting Information). This also explains that boron-nitrogen nanotubes still exhibit hydrophobicity although there are partial charges of ~0.4e on the boron nitrogen atoms[53].

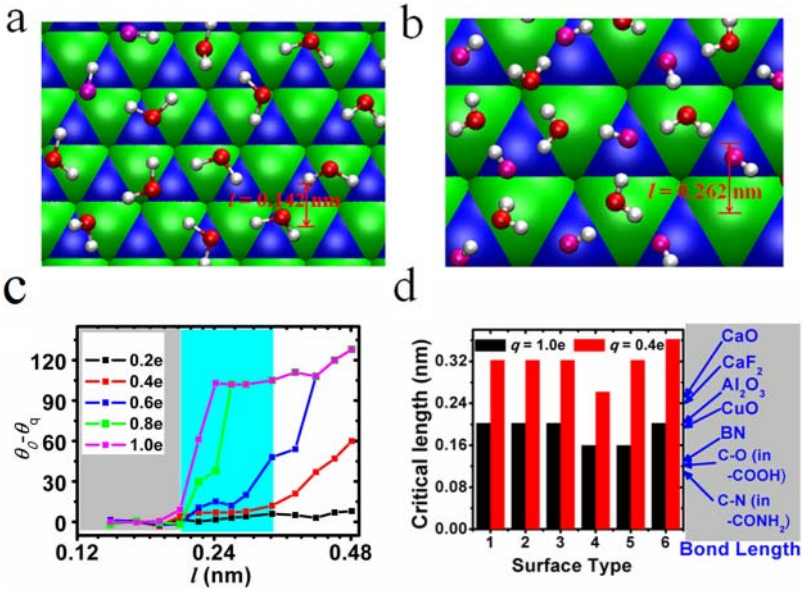

Figure 1 | Introduction to the model system and its wetting behaviour. (a,b) Structure of the model surface with $l = 0.142$ nm and 0.262 nm at $q = 1.0$ e together with snapshots of some water molecule. The green and blue triangles represent the atoms on the solid surface with positive charges and negative charges, respectively. The oxygen and hydrogen atoms of the water molecules are shown by (bright or soft) red and white spheres. The oxygen atom of a water molecule with one OH bond pointing downward is shown by soft red. (c) Contact angle discrepancy ($\theta_0 - \theta_q$) with respect to the dipole length (l) for the charge (q) 0.2 e (black), 0.4 e (red), 0.6 e (blue), 0.8 e (green), and 1.0 e (magenta). θ_q and θ_0 are the contact angles of the liquid droplets on the surface with a charge of q and without any charge, respectively. The saturation values of $\theta_0 - \theta_q$ increases from ~102° for $l = 0.242$ nm to ~130° for $l = 0.482$ nm due to the modification of the lattice length, which correspond to complete wetting of the surface ($\theta_q = 0$). (d) Critical lengths for some typical surfaces of binary compound crystals. Here, the critical length is defined as the dipole length below which the contact angle discrepancy ($\theta_0 - \theta_q$) is less than 15° for all q value in the interval of [0, 1.0 e], or in the interval of [0, 0.4 e], denoted by l_C and $l_C^{0.4}$ and shown by black and red columns, respectively. The first surface type is the structure shown in (a,b). The other surface types, increasing from 2 to 6, corresponds to the square, rhombic and rectangle lattice, (110) surface of a face-centered cube, and (110) surface of a body centered tetragonal, respectively (see Fig. S1 in Supplementary Information).

Discussions

In order to understand the mechanism underlying this behavior, we have calculated radial distribution functions (RDF) between water oxygen (O) and hydrogen (H) atoms and the surface positive and negative charged atoms, denoted as $g_{O+}(r)$, $g_{H+}(r)$, $g_{O-}(r)$ and $g_{H-}(r)$, respectively. Some typical results for $q = 0.4$ e are shown in Fig. 2. Interestingly, the RDF profiles are almost independent of the charge positivity or negativity; $g_{O+}(r) \approx g_{O-}(r)$, and $g_{H+}(r) \approx g_{H-}(r)$ for all r values when l is very small (0.142 nm). The peaks of all the RDF profiles are at $r = \sim 0.4$ nm. We have shown that the RDFs of the O and H for $q = 0$ are consistent with the RDFs for $q = 1.0$ e when $l = 0.142$ nm (see Fig. S1 in the Supporting Information). In fact, we find that the RDF profiles are almost independent of the charge for $q \leq 1.0$ e, suggesting that the dynamics of the surface water is independent of the quantity of the charge dipoles on the surface for $l = 0.142$ nm. In Fig. 1(a) we show the snapshot of the water molecules in the layer with a thickness of 0.5 nm from the top view for $l = 0.142$ nm at $q = 1.0$ e. These water molecules do not show any ordering structure, indicating that water molecules seem not "see" the surface charges even $q = 1.0$ e. The RDF profiles for $l = 0.182$ nm were quite similar to the RDF profiles for $l = 0.142$ nm. When $l = 0.222$ nm, a clear but small peak appears at $r = 0.20$ nm for $g_{H-}(r)$. At $l = 0.362$ nm, clearer peaks appears at $r \approx 0.18$ nm for $g_{H-}(r)$ profiles and at $r \approx 0.27$ nm for $g_{O-}(r)$ profiles. The two peaks become clearer for $l = 0.402$ nm. The distance between those two peaks is found to be about 0.09 nm, which is very close to the bond length of O-H in the SPC/E water model of 0.1 nm used here. Careful examination finds that most of the O atoms near the peak at $r \approx 0.27$ nm chemically bond H atoms near the peak $r \approx 0.18$ nm. This explains the observation that the peak in the RDF profile of $g_{O-}(r)$ moves towards left as l increases since the first peak of $g_{H-}(r)$ moves towards left. From the snapshot for $l = 0.262$ nm at $q = 1.0$ e shown in Fig. 1(b), one can observe that the water molecules close to the solid surface show clear structure ordering, i.e, the water molecules above the negatively charged atoms have one OH bond pointing downward to the surface, and the water molecules above the positively charged atoms have neither OH bond pointing downward, indicating that the oxygen atoms are nearest to the positively charged atoms on the surface. Thus, the water molecules on the surface with $l = 0.262$ nm behaves qualitatively different from the water molecules on the surface with $l = 0.142$ nm, consistent with the RDF profiles. There is also a peak for the RDF profile of $g_{H+}(r)$ at $r = 0.32$ nm. As l increases more, the locations of the peaks in the profile of $g_{O+}(r)$ moves towards smaller values of r, whereas the profiles of $g_{H+}(r)$ show different characteristics. All of these observations show that the charge dipoles on the sold surface have a more profound effect on the distribution of the water orientation on the solid surface when l is larger. Due to the small van de Waals radius of an H atom, H is much closer to the negative charges compared to the distance from the positive charges to O atoms.

The interactions between water molecules and the solid surface are usually regarded as the key factor in determining the wetting property of the surface. We have computed the average electrostatic interaction energy between each single charge (average value from both cases of positive and negative charges) on solid surface and all the water molecules near the charge, with respect to l for various q, denoted as $E_{electro}$ (see Fig. 3). $E_{electro}$ is very small for $l \leq l_C$ (the the grey shadows in Fig. 3). The water on the solid surface seems not to "feel" the attractive interactions from the charge on the solid surface, contrary to intuition, but consistent with our simulation results that solid surfaces with charge dipoles still exhibit hydrophobic behavior for $l \leq l_C$. As l increases from l_C, the electrostatic interaction increases monotonically. We have also computed the electrostatic interaction energies from the RDFs of water oxygen O and hydrogen H atoms, denoted by E_{theory}. Herein, the partial charges on an oxygen and hydrogen atoms are -0.8476 e and 0.4238 e, respectively, from the SPC/E water model. As shown in Fig. 3, E_{theory} agrees with $E_{electro}$ very well.

Now we may capture the physics behind this unexpected behavior. The key is the collective effect of the interaction of the water molecules with the charge dipoles on the solid surface, where the steric exclusion effect between the water molecules may become of importance. When l is large enough, the negative charges on the solid surface attract the H atoms and the positive charges attract the O atoms so that some of the H atoms are very close to the negative charges and some of the O atoms are very close to the positive charges. When l decreases to a smaller value, the steric exclusion effect prevents those hydrogen atoms from staying very close to the negative charge and those oxygen atoms from staying very close to the positive charge. The electrostatic interactions between water molecules and surface charge dipoles decrease correspondingly. When l is small enough, it becomes almost impossible to arrange the positions and orientation of the water molecules so that the O atoms are close to the positive charges while the H atoms are close to

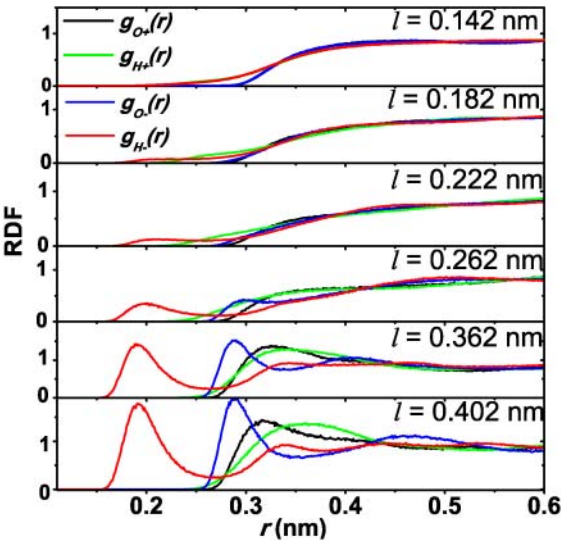

Figure 2 | Radial distribution functions (RDF) of water oxygen O and hydrogen H atoms with respect to the surface positive and negative charged atoms for the surfaces considered, respectively, for various dipole lengths l at $q = 0.4$ e. The black lines and green lines correspond to the RDF profiles for the oxygen (O) and hydrogen (H) to the positive charges, denoted by $g_{O+}(r)$ and $g_{H+}(r)$, respectively. Blue lines and red lines correspond to the RDF profiles for the oxygen (O) and hydrogen (H) to the negative charges, denoted by $g_{O-}(r)$ and $g_{H-}(r)$, respectively.

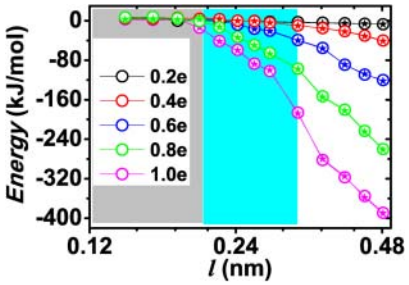

Figure 3 | Electrostatic interaction energy between water molecules and each charge on the solid surface with respect to the dipole length (l) for the charge (q) 1.0 e (magenta), 0.8 e (green), 0.6 e (blue), 0.4 e (red), and 0.2 e (black). The open circles are determined directly from numerical simulations (denoted by $E_{electro}$) and the filled stars represent the electrostatic interactions energy calculated from the radial distribution function (denoted by E_{theory}).

the negative charges. It is clear that this value of l should be comparable or smaller than the size of the water so that the positions and orientations of the water molecules near the solid surface cannot be arranged according to the charges on the surfaces. Our numerical results have shown that the critical surface dipole length l_C = 0.202 nm and $l_C^{0.4}$ = 0.302 nm are close to the diameter of a water molecule (~0.28 nm). Consequently, when $l \leq l_C$, the atom densities are almost independent of the signs and the qualities of the charges and the water molecules on the solid surface seem not to "see" the charges on the solid surface.

The existence of the critical length is universal. We have studied the wetting behavior of the surfaces of other five typical types. Three of them have 1 : 1 ratio, and the other two have 1 : 2 ratio of the number of positively charged atoms to the number of negatively charged atoms. Explicitly, the three typical types of surfaces of 1 : 1 ratio are the type 2 surface obtained from (100) surface of a face-centered cube (such as the NaCl(100) surface), the type 3 surface obtained from (110) surface of simple cube (such as the CsCl(110) surface) and the type 4 surface obtained from (110) surface of face-center cube (such as the NaCl(110) surface), which are shown in Fig. 4(a)(b)(c), respectively. The other two typical types of surfaces of 1 : 2 ratio are the type 5 surface obtained from (110) surface of a face-centered cube (such as the CaF_2(110) surface) and the type 6 surface obtained from (110) surface of a body centered tetragonal (such as the BaO_2(110) surface), as shown in Fig. 4(d)(e), respectively. For the two typical types of surfaces of 1 : 2 ratio, in order to keep the system charge neutral, we set the quantity of each positive charge twice of the quantity of each negative charge. Thus, for easy description, the notion q in the contexts below corresponds to the quantity of the positive charge for the two types of 1 : 2 ratio. The structure shown in Fig 1(a) is denoted as type 1. In Fig. 1(d), we show the critical lengths of the charge dipoles for various types of the solid surfaces. One can observe that the explicit value of the critical value depends on the geometry of the solid surface and the dipole structures. Explicitly, the critical length of the charge dipoles on the solid surface is l_C = 0.202 nm for q = 1.0 e and $l_C^{0.4}$ = 0.302 nm for q = 0.4 e for the types 1–3. For the type 4, the critical length of the charge dipoles on the solid surface is l_C = 0.162 nm for q = 1.0 e and $l_C^{0.4}$ = 0.262 nm for q = 0.4 e, which are smaller than the case of type 1–3. As for the type 5 and 6, the critical length of the charge dipoles on the solid surface is $l_C^{1.0}$ = 0.162 nm for q = 1.0 e and $l_C^{0.4}$ = 0.302 nm for q = 0.4 e; $l_C^{1.0}$ = 0.202 nm for q = 1.0 e and $l_C^{0.4}$ = 0.362 nm for q = 0.4 e, respectively. The close values of the critical lengths in the solid surfaces of the first three types may be attributed to that there is only one characteristic length for each type. For the type 4 solid surface, there are two characteristic lengths, where the longer one is $\sqrt{2}$ times larger than the shorter one. Here we only consider the shorter one as the critical length so that the critical length shows a smaller value. As for the types 5 and 6, the number of positively charged and negatively charged atoms is different and there are also two characteristic lengths so that the critical lengths show different behavior from those in the surfaces of the first three types. The lengths of the chemical bonds of some typical binary compound crystals or chemical groups are shown in Fig. 1(d), including the lengths of the C-O bond in –COOH group, C-N bond in $–CONH_2$ group, and the bonds of BN, CuO, Al_2O_3, CaF_2 and CaO. It is clear that all of them are less than $l_C^{0.4}$ and most of them are less than l_C. This demonstrates that the observations should be of general importance.

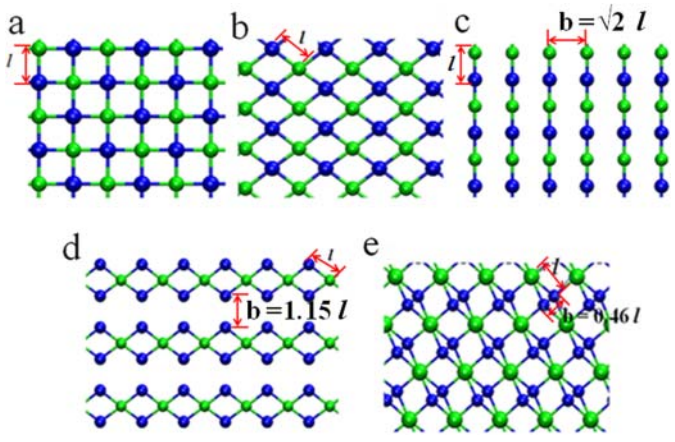

Figure 4 | Other five typical surfaces of binary compound crystals, which correspond to the surface type number = 2, 3, 4, 5 and 6, respectively. The green and blue spheres represent positively and negatively charged atoms, respectively.

In summary, we have shown that the wetting properties of a solid surface significantly depend on the surface topology parameter, which can be characterized by the length of the charge dipoles l. Counter to intuition, the length of the charge dipoles on the solid surface plays a key role on the wetting behavior and there is a critical length of the charge dipoles, below which the charge dipoles on the solid surface have a negligible role in the wetting property. The solid surface still exhibits hydrophobic behavior when the dipole length is less than the critical value, indicating that the water molecules on the solid surface seem not to "feel" attractive interactions from the charge dipoles on the solid surface, no matter how large the moment magnitude of the charge dipoles is. Those unexpected observations result from the collective interactions between the water molecules and charge dipoles on the solid surface, where the steric exclusion effect between water molecules prevents those hydrogen atoms of water molecules from staying very close to the negative charge and those oxygen atoms of water molecules from staying very close to the positive charge, reducing the interactions between the water molecules and the charge dipoles. Remarkably, the steric exclusion effect is also important for surfaces with charge dipole lengths l greater than this critical length. When charge dipole lengths are greater than this critical length, the surfaces become more hydrophilic with the dipole lengths increase. We note that the bond lengths of most of common materials are less than the critical lengths, suggesting that the observation should be of general importance to the surface wetting properties. We further note that the critical length of the surface still exists for different Lennard-Jones parameters of the atoms on the substrate within a reasonable range (see Table S2 in the Supplementary Information). Moreover, when the charge dipoles are provided from planting groups, such as –COOH, the critical values will be smaller due to the flexible behavior of the groups, which decreases the steric exclusion effect. These findings also have biological significance and are helpful for interfacial engineering, new functional material design including carbon and silicon nanostructures, and offer insights into many unexpected observations on wetting behavior.

Methods

A constant temperature and constant volume (NVT ensemble) MD simulation was performed using a time step of 1.0 fs with Gromacs 3.3.1[58]. The periodic boundary conditions were applied in all directions. The selection of a vapor-liquid coexistence system was used to maintain the ambient conditions, and a Berendsen thermostat[59] with a time constant of 1.0 ps for coupling was used to maintain the temperature of the water at 300 K. The solid atom with Lennard-Jones parameters ε_{ss} = 0.105 kcal/mol and σ_{ss} = 3.343 Å, and the SPC/E water model was used as the explicit solvent. A cutoff of 10 Å was used for both the particle-mesh Ewald method[60] with a real space to model long-range electrostatic interactions, and for the van der Waals interactions. The contact angle of a water droplet was calculated from the density profile. For simplicity, when all of the water molecules completely spread on the surface, we assumed that the contact angle was 0. In the computation of the radial distribution function (RDF) of the water molecules next to a given surface and the interaction between those water molecules and the surface, we considered the solid surface with 1664 atoms immersed in the center of a water box with 4 nm thickness of water layer, where periodic boundary conditions apply along the three dimensions[52].

1. Chandler, D. Interfaces and the driving force of hydrophobic assembly. *Nature* **437**, 640–647 (2005).

2. Han, S. H., Choi, M. Y., Kumar, P. & Stanley, H. E. Phase transitions in confined water nanofilms. *Nature Phys.* **6**, 685–689 (2010).
3. Wang, B. & Král, P. Chemically Tunable Nanoscale Propellers of Liquids. *Phys. Rev. Lett.* **98**, 266102 (2007).
4. Wang, C. L. *et al*. Stable Liquid Water Droplet on a Water Monolayer Formed at Room Temperature on Ionic Model Substrates. *Phys. Rev. Lett.* **103**, 137801 (2009).
5. Strekalova, E. G., Mazza, M. G., Stanley, H. E. & Franzese, G. Large decrease of fluctuations for supercooled water in hydrophobic nanoconfinement. *Phys. Rev. Lett.* **106**, 145701 (2011).
6. Raschke, T. M., Tsai, J. & Levitt, M. Quantification of the hydrophobic interaction by simulations of the aggregation of small hydrophobic solutes in water. *Proc. Natl. Acad. Sci. USA* **98**, 5965–5969 (2001).
7. Weiss, D. R., Raschke, T. M. & Levitt, M. How hydrophobic buckminsterfullerene affects surrounding water structure. *J. Phys. Chem. B* **112**, 2981–2990 (2008).
8. Hummer, G., Rasaiah, J. C. & Noworyta, J. P. Water conduction through the hydrophobic channel of a carbon nanotube. *Nature* **414**, 188–190 (2001).
9. Ashbaugh, H. S. & Pratt, L. R. Colloquium: Scaled particle theory and the length scales of hydrophobicity. *Rev. Mod. Phys.* **78**, 159–178 (2006).
10. Stone, H. A., Stroock, A. D. & Ajdari, A. Engineering flows in small devices microfluids towards a lab-on-a-chip. *Annu. Rev. Fluid Mech* **36**, 381 (2004).
11. Zhu, Y. & Granick, S. Rate-dependent slip of newtonian liquid at smooth surfaces. *Phys. Rev. Lett.* **87**, 096105 (2001).
12. Briscoe, W. H. *et al*. Boundary lubrication under water. *Nature* **444**, 191–194 (2006).
13. Meng, S., Zhang, Z. Y. & Kaxiras, E. Tuning solid surfaces from hydrophobic to superhydrophilic by submonolayer surface modification. *Phys. Rev. Lett.* **97**, 036107 (2006).
14. Sedlmeier, F., Horinek, D. & Netz, R. R. Nanoroughness, Intrinsic Density Profile, and Rigidity of the Air-Water Interface. *Phys. Rev. Lett.* **103**, 136102 (2009).
15. Ogasawara, H. *et al*. Structure and bonding of water on Pt(111). *Phys. Rev. Lett.* **89**, 276102 (2002).
16. Huang, D. M., Sendner, C., Horinek, D., Netz, R. R. & Bocquet, L. Water Slippage versus Contact Angle: A Quasiuniversal Relationship. *Phys. Rev. Lett.* **101**, 226101 (2008).
17. Li, J. Y. *et al*. Electrostatic gating of a nanometer water channel. *Proc. Natl. Acad. Sci. USA* **104**, 3687–3692 (2007).
18. Yuan, Q. Z. & Zhao, Y. P. Precursor Film in Dynamic Wetting, Electrowetting, and Electro-Elasto-Capillarity. *Phys. Rev. Lett.* **104**, 246101 (2010).
19. Yang, J. J., Meng, S., Xu, L. F. & Wang, E. G. Water adsorption on hydroxylated silica surfaces studied using the density functional theory. *Phys. Rev. B* **71**, 035413 (2005).
20. Meng, X. W., Wang, Y., Zhao, Y. J. & Huang, J. P. Gating of a Water Nanochannel Driven by Dipolar Molecules. *J. Phys. Chem. B* **115**, 4768–4773 (2011).
21. Verdaguer, A., Sacha, G. M., Bluhm, H. & Salmeron, M. Molecular structure of water at interfaces: Wetting at the nanometer scale. *Chem Rev* **106**, 1478–1510 (2006).
22. Ball, P. Water as an active constituent in cell biology. *Chem Rev* **108**, 74–108 (2008).
23. Godawat, R., Jamadagni, S. N. & Garde, S. Characterizing hydrophobicity of interfaces by using cavity formation, solute binding, and water correlations. *Proc. Natl. Acad. Sci. USA* **106**, 15119–15124 (2009).
24. Koishi, T., Yasuoka, K., Fujikawa, S., Ebisuzaki, T. & Zeng, X. C. Coexistence and transition between Cassie and Wenzel state on pillared hydrophobic surface. *Proc. Natl. Acad. Sci. USA* **106**, 8435–8440 (2009).
25. Gu, W. *et al*. Design of a gated molecular proton channel. *Angew. Chem. Int. Ed.* **50**, 768–771 (2010).
26. Das, P. & Zhou, R. H. Urea-Induced Drying of Carbon Nanotubes Suggests Existence of a Dry Globule-like Transient State During Chemical Denaturation of Proteins. *J. Phys. Chem. B* **114**, 5427 (2010).
27. Janecek, J. & Netz, R. R. Interfacial water at hydrophobic and hydrophilic surfaces: Depletion versus adsorption. *Langmuir* **23**, 8417–8429 (2007).
28. Tajkhorshid, E. *et al*. Control of the Selectivity in the AQP Water Channel Family by Global Orientational Tuning. *Science* **296**, 525–530 (2002).
29. Raschke, T. M. Water structure and interactions with protein surfaces. *Curr. Opin. Struct. Biol.* **16**, 152–159 (2006).
30. Cheung, M. S., Garcia, A. E. & Onuchic, J. N. Protein folding mediated by solvation: Water expulsion and formation of the hydrophobic core occur after the structural collapse. *Proc.Natl. Acad. Sci. USA* **99**, 685–690 (2002).
31. VanVeen, H. W. *et al*. Multidrug resistance mediated by a bacterial homolog of the human multidrug transporter MDR1. *Proc. Natl. Acad. Sci. USA* **93**, 10668–10672 (1996).
32. Wimley, W. C. & White, S. H. Experimentally determined hydrophobicity scale for proteins at membrane interfaces. *Nature Struct. Biol.* **3**, 842–848 (1996).
33. Titov, A. V., Kral, P. & Pearson, R. Sandwiched Graphene-Membrane Superstructures. *ACS Nano* **4**, 229–234 (2010).
34. Bocquet, L. & Charlaix, E. Nanofluidics, from bulk to interfaces. *Chem. Soc. Rev.* **39**, 1073–1095 (2010).
35. Whitby, M. & Quirke, N. Fluid flow in carbon nanotubes and nanopipes. *Nature Nanotech.* **2**, 87–94 (2007).
36. Squires, T. M. & Quake, S. R. Microfluidics: fluid physics at the nanoliter scale. *Rev. Mod. Phys.* **77**, 977 (2005).
37. Besteman, K., Lee, J. O., Wiertz, F. G. M., Heering, H. A. & Dekker, C. Enzyme-coated carbon nanotubes as single-molecule biosensors. *Nano Lett.* **3**, 727–730 (2003).
38. Shea, J. E., Onuchic, J. N. & Brooks, C. L. Probing the folding free energy landscape of the src-SH3 protein domain. *Proc. Natl. Acad. Sci. USA* **99**, 16064–16068 (2002).
39. Zhou, R. H., Huang, X. H., Margulis, C. J. & Berne, B. J. Hydrophobic collapse in multidomain protein folding. *Science* **305**, 1605–1609 (2004).
40. Hua, L., Huang, X., Liu, P., Zhou, R. & Berne, B. J. Nanoscale Dewetting Transition in Protein Complex Folding. *J. Phys. Chem. B* **111**, 9069–9077 (2007).
41. Berne, B. J., Weeks, J. D. & Zhou, R. H. Dewetting and Hydrophobic Interaction in Physical and Biological Systems. *Annu. Rev. Phys. Chem.* **60**, 85–103 (2009).
42. Li, J. Y. *et al*. Hydration and dewetting near graphite-CH3 and graphite-COOH plates. *J. Phys. Chem. B* **109**, 13639–13648, doi:10.1021/jp044090w (2005).
43. Huang, X., Margulis, C. J. & Berne, B. J. Dewetting-induced collapse of hydrophobic particles. *Proc. Natl. Acad. Sci. USA* **100**, 11953–11958 (2003).
44. Charles, T. Hydrophobic free energy, micelle formation and the association of proteins with amphiphiles. *J. Mol. Bio.* **67**, 59–74, doi:10.1016/0022-2836(72)90386-5 (1972).
45. Israelachvili, J. N., Mitchell, D. J. & Ninham, B. W. Theory of self-assembly of hydrocarbon amphiphiles into micelles and bilayers. *Journal of the Chemical Society, Faraday Transactions 2: Molecular and Chemical Physics* **72**, 1525–1568 (1976).
46. Wang, H. J., Xi, X. K., Kleinhammes, A. & Wu, Y. Temperature-induced hydrophobic-hydrophilic transition observed by water adsorption. *Science* **322**, 80–83 (2008).
47. Cheng, Y. K. & Rossky, P. J. Surface topography dependence of biomolecular hydrophobic hydration. *Nature* **392**, 696–699 (1998).
48. Zangi, R. & Berne, B. J. Aggregation and dispersion of small hydrophobic particles in aqueous electrolyte solutions. *J. Phys. Chem. B* **110**, 22736–22741 (2006).
49. Zangi, R., Hagen, M. & Berne, B. J. Effect of ions on the hydrophobic interaction between two plates. *J. Am. Chem. Soc.* **129**, 4678–4686 (2007).
50. Giovambattista, N., Debenedetti, P. G. & Rossky, P. J. Effect of surface polarity on water contact angle and interfacial hydration structure. *J. Phys. Chem. B* **111**, 9581–9587 (2007).
51. Giovambattista, N., Lopez, C. F., Rossky, P. J. & Debenedetti, P. G. Hydrophobicity of protein surfaces: Separating geometry from chemistry. *Proc.Natl. Acad. Sci. USA* **105**, 2274–2279 (2008).
52. Giovambattista, N., Debenedetti, P. G. & Rossky, P. J. Enhanced surface hydrophobicity by coupling of surface polarity and topography. *Proc. Natl. Acad. Sci. USA* **106**, 15181–15185 (2009).
53. Won, C. Y. & Aluru, N. R. Structure and dynamics of water confined in a boron nitride nanotube. *J. Phys. Chem. C* **112**, 1812–1818 (2008).
54. Golberg, D., Bando, Y., Tang, C. C. & Zhi, C. Y. Boron nitride nanotubes. *Adv Mater* **19**, 2413–2432 (2007).
55. Li, X., Li, J. Y., Eleftheriou, M. & Zhou, R. H. Hydration and dewetting near fluorinated superhydrophobic plates. *J. Am. Chem. Soc.* **128**, 12439–12447 (2006).
56. Wang, C. L., Zhou, B., Xiu, P. & Fang, H. P. Effect of Surface Morphology on the Ordered Water Layer at Room Temperature. *J. Phys. Chem. C* **115**, 3018–3024 (2011).
57. James, M. *et al*. Nanoscale condensation of water on self-assembled monolayers. *Soft Matter* **7**, 5309–5318 (2011).
58. Lindahl, E., Hess, B. & van der Spoel, D. GROMACS 3.0: a package for molecular simulation and trajectory analysis. *J. Mol. Model.* **7**, 306–317 (2001).
59. Berendsen, H. J. C., Grigera, J. R. & Straatsma, T. P. The missing term in effective pair potentials. *J. Phys. Chem.* **91**, 6269–6271 (1987).
60. Darden, T., York, D. & Pedersen, L. Particle mesh ewald - an N.LOG(N) method for ewald sums in large systems. *J. Chem. Phys.* **98**, 10089–10092 (1993).

Acknowledgements

We gratefully acknowledge Drs. Ruhong Zhou, Yi Gao, Guanghong Zuo and Rongzheng Wan for their helpful discussions. This work was supported by the National Science Foundation of China under grant No. 10825520 and 11105088, the National Basic Research Program of China under grant No. 2012CB932400, Shanghai Leading Academic Discipline Project (B111), E-Institutes of Shanghai Municipal Education Commission, the Knowledge Innovation Program of the Chinese Academy of Sciences, Innovation Program of Shanghai Municipal Education Commission (No. 11YZ20), China Postdoctoral Science Foundation (No. 20100480645), Shanghai Postdoctoral Scientific Program (No. 11R21418100) and Shanghai Supercomputer Center of China.

Author contributions

C.L.W. performed most of the numerical simulations. H.P.F. and C.L.W. carried out most of the theoretical analysis. B.Z., Y.S.T., M.Y.D. and P.X. carried out some numerical simulations and theoretical analysis. H.P.F, C.L.W. and J.Y.L. contributed most of the ideas and wrote the paper. All authors discussed the results and commented on the manuscript.

Additional information

Supplementary information accompanies this paper at http://www.nature.com/scientificreports

Competing financial interests: The authors declare no competing financial interests.

How to cite this article: Wang, C. *et al.* Critical Dipole Length for the Wetting Transition Due to Collective Water-dipoles Interactions. *Sci. Rep.* **2**, 358; DOI:10.1038/srep00358 (2012).